Electron Holography and AFM Studies on Styrenic Block Copolymers and a High Impact Polystyrene

Paul Simon,[1] Rameshwar Adhikari,[2] Hannes Lichte,[1] Goerg H. Michler,[2] Marc Langela[3]

[1]*Institute of Structure Physics, Technical University Dresden, Zellescher Weg 16, D - 01062 Dresden, Germany, and Triebenberg Laboratory, Technical University Dresden, Zum Triebenberg 50, D-01474 Schönfeld-Weissig, Germany*
[2]*Institute of Materials Science, Department of Engineering, University of Halle-Wittenberg, D-06099 Halle/Saale Germany*
[3]*polyMaterials AG, Innovapark 20, D-87600 Kaufbeuren, Germany*

Received 24 February 2004; accepted 14 September 2004
DOI 10.1002/app.21600
Published online in Wiley InterScience (www.interscience.wiley.com).

ABSTRACT: Many of the artifacts of conventional electron microscopy can be avoided if the unstained polymers are studied by electron holography and atomic force microscopy (AFM). Holograms of thin sections (50–70 nm) of organic block copolymers were recorded, and the corresponding phase images were reconstructed. In this way, typical structures such as lamellae and cylinders could be imaged without any staining. In addition, we successfully recorded holograms and performed Lorentz microscopy of an impact-modified polystyrene (high-impact polystyrene). The results were compared with the tapping mode AFM phase images. Electron holography and AFM have been demonstrated as suitable tools to image unstained heterogeneous polymers, leading to the understanding of their structure. © 2005 Wiley Periodicals, Inc. J Appl Polym Sci 96: 1573–1583, 2005

Key words: atomic force microscopy (AFM); transmission electron microscopy (TEM); electron holography; block copolymers; polymer blends

INTRODUCTION

Imaging of low atomic number compounds, the so called weak phase objects, still poses a severe challenge to conventional electron microscopy. For organic objects, besides the low contrast, beam sensitivity causes the main restriction to imaging techniques. Organic polymers show explicit sensitivity to beam damage as a consequence of inelastic interactions. Therefore, the resolution will finally be controlled by the critical dose. Already in the very beginning of electron microscopy several methods were developed to overcome these difficulties. Chemical staining and defocus are the most commonly used techniques for weak phase objects. Recently, low voltage microscopy has shown promising results despite the requirement of very thin samples.[1] Other promising methods, which do not need staining, are energy-filtered elemental mapping by electron energy loss spectroscopy (EELS) and, especially for crystalline samples, dark field imaging using scattering contrast.

A new approach for imaging the microstructure of multicomponent polymers by transmission electron microscopy (TEM) is provided by electron holography. It uses the idea to conserve the phase information of the object and thus to reproduce even a small variation of densities or chemical composition occurring within the sample.[2] In electron holography, the images produced are the two-dimensional (2D) projections of thin (but 3D) specimens. Besides holography, there are other phase recovery methods, such as the focus variation technique, which proved to be successful for imaging, e.g., single doping atoms inside of carbon nanotubes.[3] Electron holography is widely used in materials science to display electric or magnetic fields.[4–8] However, there are only a limited number of publications on electron holography of polymers.[2,9–12] One reason for this is the explicit beam sensitivity of organic samples. Moreover, chemistry research may have been informed insufficiently about the opportunities offered by electron holography.

In recent years, the atomic force microscope (AFM) has been extensively employed to investigate the morphology of various polymers. The "tapping mode" of the AFM offers attractive possibilities of imaging structures and properties of heterogeneous polymers. A growing number of publications prove the AFM is an advanced microscopic tool for mapping the surface topography and the composition of heterogeneous polymer systems, including block copolymers.[13–23] This work is aimed at the investigation of weak phase heterogeneous organic materials by Lorentz micros-

Correspondence to: P. Simon (simon@cpfs.mpg.de).
Present address for P. Simon: Max Planck Institute for Chemical Physics of Solids, Nöthnitzer Str. 40, 01187 Dresden, Germany.

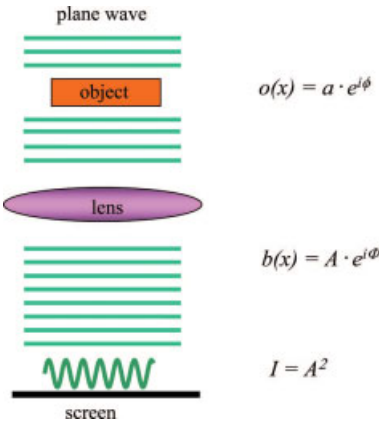

Figure 1 Scheme showing the functioning of conventional electron microscopy: phase information Φ is partially lost.

copy and electron holography and comparison of the results with those obtained with AFM.

Contrast formation of weak phase objects in the electron microscope

In general, the electron wave leaving an object ("object exit wave") is modulated by the elastic interaction in amplitude a and phase φ. In conventional electron microscopy, the image intensity $I(x) = b(x)b'(x) = A^2(x)$ is recorded, whereas the image phase $\Phi(x)$ is lost (Fig. 1). Therefore, by means of a suitable defocus, the object phase $\varphi(x)$ has to be directed into the image amplitude $A(x)$ to be recordable at a sufficient contrast. If the structures of interest are larger extended than the atomic details (e.g., polymers), one has to apply a much stronger underfocus to visualize them with a sufficient contrast. This, however, produces artifacts such as delocalization and further causes deterioration of resolution.

In conventional electron microscopy the structures of weak phase objects are visualized mainly by either chemical staining or defocus. In the following section, we discuss the imaging and contrast formation using the conventional defocus technique and compare it with electron holography.

Lorentz microscopy

We applied the Lorentz lenses instead of the conventional objective lens to enhance the contrast. The so-called Lorentz (or TWIN 2) lens is a minilens in the lower pole piece of the objective lens. It was primarily designed for high-contrast imaging of magnetic and biological specimens and has a theoretical point resolution of about 2.2 nm. The focal length of the TWIN2 lens is approximately 12 times larger and the spherical aberration is about 6,000 times higher than that of the conventional "Super Twin" objective lens.

For Lorentz microscopy it is still essential to defocus to gain sufficient contrast for large area objects. Using the defocus technique, the transfer of the object phase into the amplitude of the image can be optimized. Large area objects display poor contrast at small defocus. Hence, we have to defocus strongly to image large area objects.[24] If we defocus strongly, the spacings of interest are transferred with a sufficient contrast but will cause a remarkable loss of resolution for finer spacings. At strong underfocus, the appearance of Fresnel fringes at the edges of the sample make the image interpretation quite difficult. The defocus technique was first applied by Petermann et al.[25] in 1975 for polymers, and, later on, it proved to be successful also for block copolymers in 1983.[26]

Holography

The difficulties of imaging weak phase objects by means of conventional electron microscopy give rise to the question of whether it is possible to achieve additional information by electron holography. In holography, both phase and amplitude of the image wave are transferred simultaneously.

The illuminating wave is divided in two parts, i.e., the object and reference wave. The object wave propagates through the object and is modulated in amplitude and phase according to the object structure. The reference wave goes through a vacuum and is not affected by the object. The electron biprism, which is a positively charged wire, superimposes both the object and reference waves in the image plane, giving rise to an interference pattern, the so-called hologram (Figs. 2 and 3). The biprism is arranged between the objective lens and the first intermediate image. To achieve a high contrast of the hologram fringes, hence, as good signal/noise ratio in the reconstructed wave, a monochromatic and coherent illumination as provided by a field emission gun is indispensable.

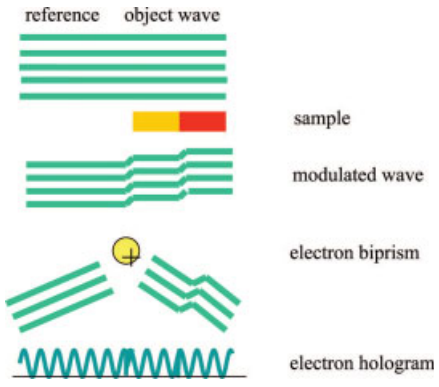

Figure 2 Principle of holography: phase of image wave is recorded by means of interference with reference wave.

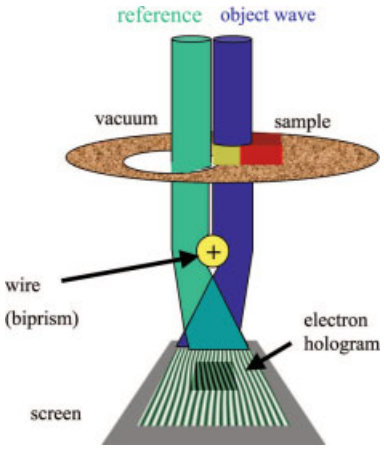

Figure 3 Off-axis electron holography set up: the reference wave is running through vacuum and is thus not affected by the object.

After magnification by means of the subsequent lenses, the hologram is recorded by a CCD camera. The digitized image is transferred to a computer where amplitude and phase of the recorded wave can be reconstructed separately by means of numerical image processing. Both amplitude image and phase image of the image wave are reconstructed in real space.[27]

A big advantage of holography is that even a very small phase shift in the sample can be detected without any treatment of the sample (e.g., staining) or the microscope parameters (e.g., defocus, low voltage).

In the case of low atomic number elements like carbon and hydrogen or thin layers, the interaction between the electrons and the sample is weak. As a consequence, the induced phase shift φ of the incident plane electron wave, which is given by the product of sample thickness d and mean inner potential U, will also be rather small and therefore provides poor contrast. Therefore, one would anticipate that a larger sample thickness would be useful for holography. The thicker the sample, the more phase shift is accumulated as illustrated in Figure 4. However, increasing thickness has a consequence of increased inelastic scattering. Inelastically scattered electrons are not coherent with the reference wave, thus destroying contrast by producing noisy underground of the signal. Consequently, one has to optimize the sample thickness to maximize the signal/noise ratio of the recorded wave and produce a measurable phase shift, simultaneously minimizing the inelastic scattering.

Atomic force microscopy (AFM)

Surface analysis of polymeric materials with the AFM is a very rapidly growing area of research. Several AFM techniques have been developed to achieve material contrast in heterogeneous polymers. Tapping mode is the most gentle AFM technique which is especially suited for the polymers investigated in this work with respect to their soft nature. In this work, we limit our discussion mainly to the tapping mode phase data collected under moderate tapping forces. This means that the ratio of amplitude of interacting cantilever to that of the free oscillation (i.e., set point ratio) was set to approximately 0.8.

The heterogeneous polymers (both block copolymers and high-impact polystyrene, HIPS) included in this work consist of hard polystyrene (PS) and soft polydienes (polyisoprene, PI; polybutadiene, PB), or ethylene/butylene copolymer (EB), which form high and low modulus phases, respectively. It has been established that, under soft and moderate tapping force, the lighter phase signal is caused by the interaction of the cantilever with high modulus domains. Conversely, the darker phase signal should correspond to the low modulus domains. Additionally, the height data collected under hard tapping allows one to qualitatively estimate the harder and the softer domains.[20,28] In this way high-phase (PS) and low-phase (PB or PI) domains in the AFM data can be easily identified.

Additionally, the phase data can be compared to the topographical data in which the domains having lower surface energy dominate the film surface protruding more to the surface.[15] It may help in identifying the domains with respect to the differences in surface energy of the components.

Furthermore, as discussed in the literature, the sample surface can be treated with a suitable solvent vapor so that one of the components is preferentially swollen. When the lower solubility phase solidifies, the higher solubility phase still contains some solvent. The more soluble phase will therefore continue to shrink on complete removal of solvent. As a result, lower solubility phase protrudes over the higher solubility phase.[16] By analyzing the AFM data, the protruded domains can be easily identified.

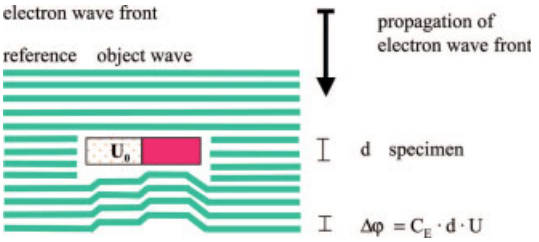

Figure 4 Phase shift $\Delta\varphi$ depends on the sample thickness d and the mean inner potential U of the specimen.

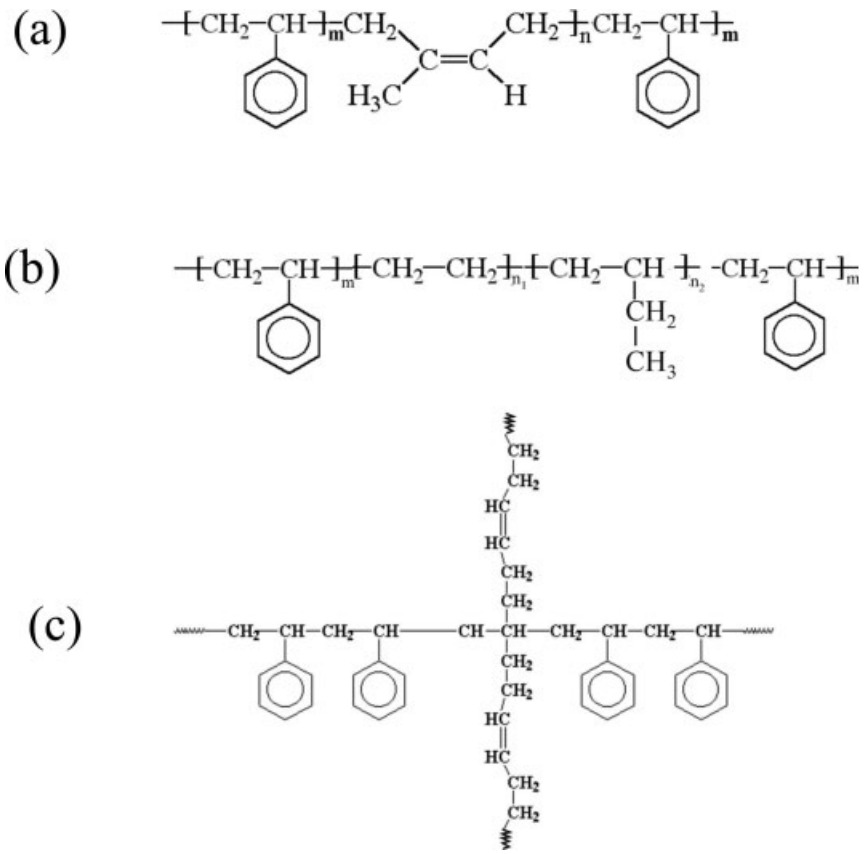

Figure 5 Schemes showing the chemical structure of the samples investigated: (a) polystyrene-*block*-polyisoprene-*block*-polystyrene copolymer (SIS-S50); (b) polystyrene-*block*-poly(ethylene/butylene)-*block*-polystyrene copolymer (SEBS-S30); and (c) high-impact polystyrene (HIPS).

EXPERIMENTAL

Materials

The materials investigated were three different heterogeneous styrene-based polymers consisting of harder and softer components: two block copolymers and an impact-modified PS the so-called HIPS.[29,30] In the electron microscope, these materials are weak phase objects and, in addition, show explicit beam sensitivity.

Block copolymers (SIS-S50 and SEBS-S30)

As block copolymers we have chosen two different rubber-toughened polystyrenes named SIS-S50 and SEBS-S30, where S50 and S30 stand for total polystyrene volume fraction present in these copolymers. The first is a linear polystyrene-*block*-polyisoprene-*block*-polystyrene SIS triblock copolymer with volume fraction of polystyrene $\phi_{PS} = 0.50$, number average molecular weight M_n = 131,200 g/mol, and $M_w/M_n = 1.04$. In Figure 5(a) the chemical structure of SIS-S50 is sketched.

As the second block copolymer sample, we have chosen a commercially available hydrogenated (completely hydrogenated polybutadiene component) polystyrene-*block*-polybutadiene-*block*-polystyrene (SBS) triblock copolymer [Fig. 5(b)] with about 30% of polystyrene (Kraton G-Polymer, Shell Chemicals). Therefore, this copolymer contains EB copolymer as the middle block and has been named SEBS-S30 ($\phi_{PS} = 0.30$, molecular weight of about 90,000 g/mol).

Styrene/diene block copolymers (with butadiene or isoprene as dienes) represent microphase-separated systems having highly ordered self-assembled structures (such as spheres, cylinders, lamellae, etc.) whose periodicity lies in the range of radius of gyration R_g of copolymer molecules. Since the dimension of phase-separated structures is well below the wave length of visible light, the products are transparent and hence find applications as packaging films. Through the variation of composition and molecular parameters, the block copolymers offer the possibility of tailoring their mechanical properties.

High-impact polystyrene (HIPS)

As the third sample we investigated HIPS with an approximately 92 wt % of polystyrene. In Figure 5(c) the chemical structure of HIPS is shown. The polystyrene matrix contains polybutadiene particles with

polystyrene inclusions giving rise to the so-called "salami" structure.[29]

Sample preparation

SIS-S50 and SEBS-S30 samples were produced by solution casting using toluene as solvent whereas HIPS was prepared by compression molding. Thin sectioning by means of an ultramicrotome allows one to obtain thin films of bulk materials. Ultrathin sections of the samples (~ 50–70 nm) were prepared using an ultramicrotome (Leica, Ultracut UCT equipped with cooling chamber operated at –120°C) with a diamond knife (Diatome company) for the TEM investigations. The thin sections about 0.2 × 0.2 mm^2 in size were spread on Cu grids without support film. The thin sections were coated with approximately 5-nm-thick carbon film to avoid charging of the specimen. The holograms were taken at the edges of the specimen, since the holographic reference beam must run through vacuum next to the sample.

After sectioning the ultrathin sections of each sample under cryogenic conditions for TEM, the remaining block of the specimen was carefully removed from the ultramicrotome and investigated by the AFM.

Microscopic techniques

A Philips CM200 FEG/ST-Lorentz electron microscope equipped with a field emission gun (FEG) operated at an acceleration voltage of 200 kV was used for the electron microscopic investigations. The Lorentz mode was found especially favorable, yielding a larger field of view for the investigation of the polymer. In the case of SIS-S50, for example, we used a magnification of ×45,000 yielding a field of view of about (540 nm^2). The applied biprism voltage of about 90 V results in a hologram fringe spacing of about 5.2 nm. The double fringe spacing of 10.4 nm gives the resolution limit of the reconstructed phase image of the recorded electron hologram.

Special precautions against beam damage (such as the use of low-dose technique or cooling stage) were not yet taken. Micrographs and holograms were recorded with a 1k*k CCD-camera and fed to a computer for on-line image processing and reconstruction nearly in real-time (Digital Micrograph 3.3.1., Gatan Company, USA). In addition to each hologram of a specimen, an "empty hologram" without any object was recorded for subsequent correction of the geometric distortion of the fringes stemming from the projection lenses and the CCD camera. Without this correction, the geometric distortions would be interpreted as large area phase shifts due to the object. Additionally, this correction largely eliminates the Fresnel fringes evoked by the biprism.

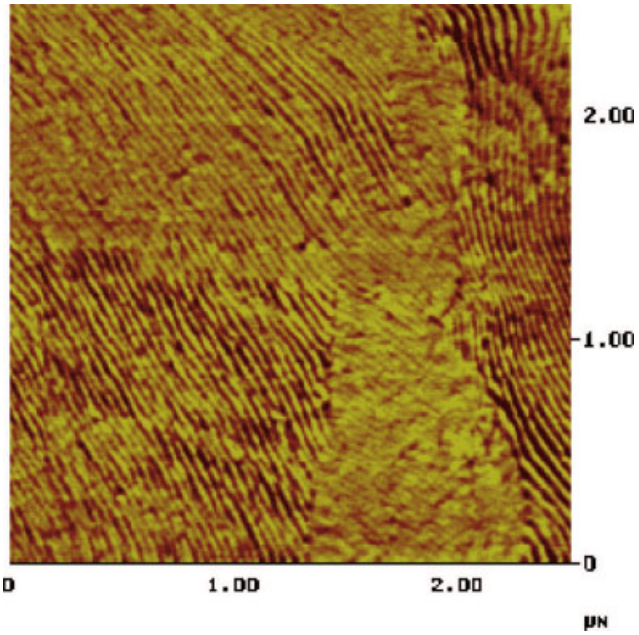

Figure 6 AFM phase image showing the bulk morphology of the polystyrene-*block*-polyisoprene-*block*-polystyrene copolymer (SIS-S50) with a lamellar periodicity of about 37 nm.

Atomic force microscope of the type MultiMode equipped with the Nanoscope IIIa controller (Digital Instruments, USA) was used to study the microstructures of the samples without staining.

The ultramicrotomed block of each sample was mounted onto the sample holder in such a way that the cut surface was parallel to the microscope head and the cut surface was scanned in tapping mode using silicon cantilevers (resonant frequency ~ 450 kHz, spring constant ~ 15 m/N) with a scan speed of approximately 1 Hz. Solution cast thin films of block copolymers were also investigated for comparison. We present the tapping mode phase images of the samples collected under moderate forces in which dark and light signals should correspond to soft (here PI, PB, or EB copolymer) and hard (here PS) polymers, respectively.

RESULTS

In order to compare the results of conventional electron microscopy and electron holography, the polymer samples were investigated by the AFM in tapping mode, collecting the height and the phase images of the samples under moderate tapping forces.

In Figure 6, one recognizes typical lamellar structure of the styrene/isoprene block copolymer (SIS-S50) sample in the AFM phase image with a lamellar spacing of about 37 nm. The equivalent lamellar structure of the sample may also be noticed in the TEM micrographs recorded in Lorentz mode at strong de-

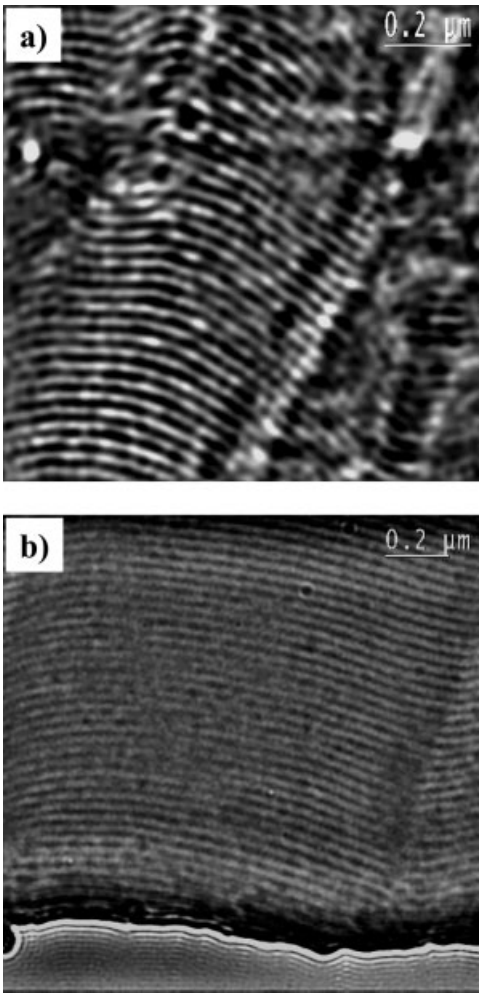

Figure 7 (a) Lorentz micrographs of polystyrene-*block*-polyisoprene-*block*-polystyrene copolymer (SIS-S50) with a lamellar periodicity of about 34–36 nm (a) and 34 nm (b).

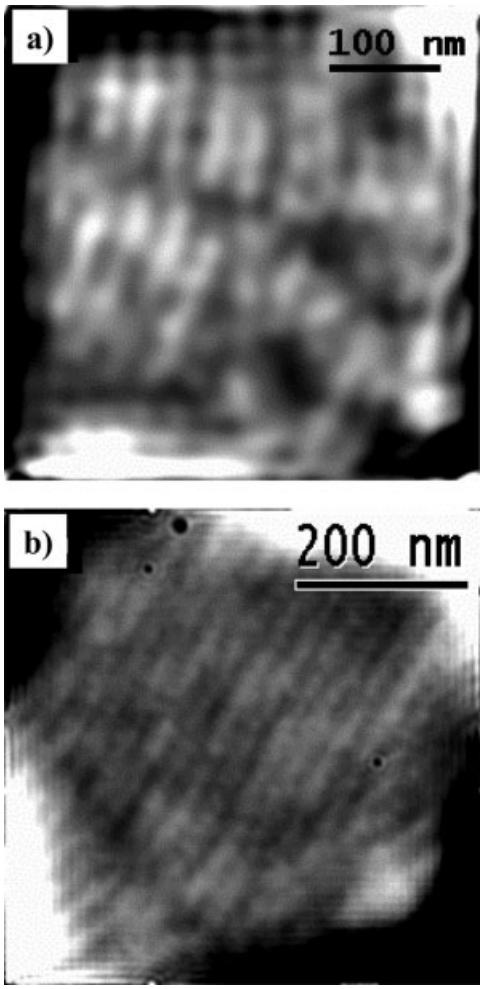

Figure 8 Electron phase images reconstructed from electron holograms of polystyrene-*block*-polyisoprene-*block*-polystyrene copolymer (SIS-S50) with lamellar periodicity of about 29 nm (a) and 31 nm (b).

focus of some tenth of micron [Fig. 7(a) and (b)]. The lamellae have a periodicity of about 34–36 nm, which is in good agreement with the value measured by the AFM (see Table I).

In Figure 8(a) and (b) the reconstructed phase images of unstained styrene/isoprene block copolymer (SIS-S50) are shown. Lamellae are running from the top to the bottom of the phase image with lamellar spacing of 29 and 31 nm. These values are in close agreement with those measured by AFM. Due to the superb large-area-contrast properties of holography in Lorentz mode, unwanted larger area structures like thickness variations caused, for example, by ultramicrotomy also are manifested in the height contrast [Fig. 8(b)]. The internal details of the polymer structure may be clearly noticed despite the lowered contrast in the phase images. The dose applied to record a hologram of the block copolymer amounted to about 300 electrons/pixel at a magnification of $\times$60,400 according to 18 e/Å^2. This value is in the range of the critical dose given for polystyrene.[24,31] The resolution of the electron phase image amounts to about 11 nm as given by the double fringe spacing of the hologram.

It is well known that the polymeric materials may suffer unwanted beam damage during the electron microscopic investigations. Since we obtained similar results from AFM and TEM measurements, and since the critical dose of PS was not exceeded, no pronounced impact of beam damage can be assumed.

As the second sample, we investigated SEBS-S30, a linear copolymer containing 30 vol % of polystyrene.

TABLE I
Microdomain Spacing in Different Block Copolymer Samples Measured by Different Techniques

Sample notation	AFM (nm)	Lorenz TEM (nm)	Holography (nm)
SIS-S50	37	34–36	31–29
SEBS-S30	26	28	—

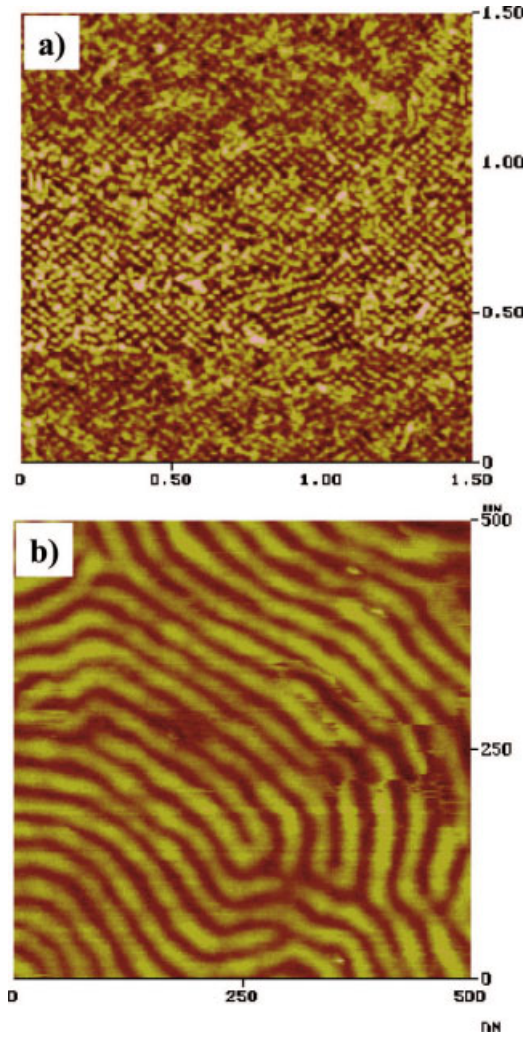

Figure 9 AFM phase image of the polystyrene-*block*-poly(ethylene/butylene)-*block*-polystyrene (SEBS) copolymer with hexagonal ordering of light PS cylinders with periodicity of about 26 nm for the bulk sample (a) and 28 nm of thin film surface (b).

In this composition, PS cylinders in EB matrix may be expected according to the classical block copolymer phase diagram. AFM investigations revealed two different phase formations [Fig. 9(a) and (b)]. Besides the hexagonal lattice of light polystyrene domains in dark ethylene/butylene copolymer matrix [Fig. 9(a)], cylinders parallel to the surface [Fig. 9(b)] also appear. The average spacing of the cylindrical microdomains is approximately 26 nm (see Table I). TEM experiments of the sample recorded in Lorentz mode at strong defocus (Fig. 10) show a spacing of $\sim$ 28 nm for the slightly tilted hexagonal arrangement.

For the HIPS the AFM phase images are shown in Figure 11(a) and (b). Typical salami structure with the rubber particles having complex internal morphology embedded in the polystyrene matrix is visible. A three-dimensional impression of the structures is presented by the surface plotting of the AFM height image [Fig. 11(b)], where the rubbery phase appears as dark deeper regions compared to the surrounding matrix. This image illustrates that the bright polystyrene particles found embedded in the rubber phase have a spherical shape.

In Lorentz microscopy, similar structures appear [Fig. 12(a) and (b)]. The comparison between electron holography and Lorentz microscopy is presented in Figure 13(a) and (b) by imaging exactly the same sample area. Apparently, Lorentz microscopy gives a superb contrast [Fig. 13(a)] of the two different polymer components. However, in the Lorentz micrograph, the imaged structures are blurred by the strong defocus and as a consequence we obtain mixed information of the microscope and sample characteristics. It is not clear which area is represented by PS and PB due to contrast inversion. In the phase image of the reconstructed hologram [Fig. 13(b)], no more Fresnel fringes are visible despite weaker contrast. In this way, we obtain the pure sample information and avoid contrast changes due to the Lorentz lens phase contrast transfer function characteristics.[32,33] In Figure 14(a), the bright polystyrene inclusions are clearly visible, separated by narrow darker regions of butadiene. In the case of the conventional Lorentz micrograph of about the same area, we find strong blurring clearly visible at the edge of the specimen [Fig. 14(b)].

The phase shift caused by the different components could be determined in this phase image since there is a vacuum as reference area beneath the sample. The shift for polystyrene amounts to 1.9 rad [Fig. 14(a)

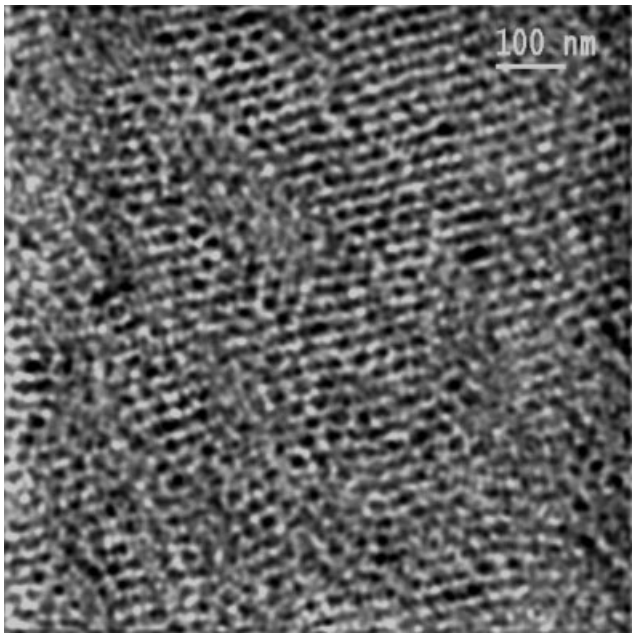

Figure 10 Overview electron micrograph of unstained polystyrene-*block*-poly(ethylene/butylene)-*block*- polystyrene (SEBS) copolymer sample recorded in Lorentz mode with domain spacing of about 28 nm.

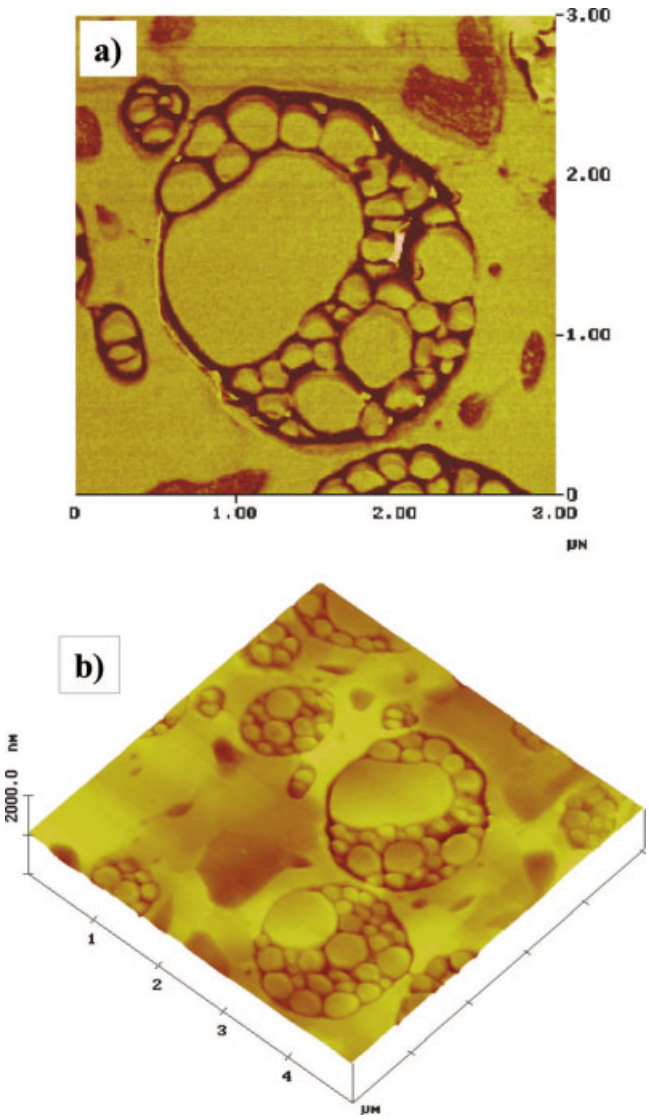

Figure 11 AFM phase image of the bulk high impact polystyrene (HIPS) sample (a) and surface plot of a part of AFM height data representing a 3D overview (b).

inset] plus 2π, which results in a thickness of about 137 nm, assuming the inner potential to be 8.2 V.[10] For polybutadiene we obtain about 40 nm thickness taking into account the density difference of about 15% between PS and PB.

To obtain the micrographs in this quality, it is essential to process the phase images under numerical reconstruction. Mainly the following three techniques were applied: with a phase wedge it is possible to eliminate strong thickness differences in the sample, phase jumps greater than 2π can be removed ("phase unwrapping"), and the phases can be shifted by an offset.

DISCUSSION AND CONCLUSION

It has been demonstrated that electron holography is a feasible tool to image weak phase structures of beam-sensitive polymers. The striking advantage of electron holography in contrast to conventional electron microscopy techniques is given by the preserved phase information. Neither staining nor defocus are needed to image weak phase objects. In this way, artifacts may be avoided, but not the limitations posed by beam sensitivity and inelastic scattering or charging effects.

AFM has been shown to be a smart and suitable method for imaging polymer superstructure in tapping mode. None of the artifacts that may be encountered in electron microscopy (e.g., effects of electron beam damage or staining of the polymer) has to be considered. In the case of SIS-S50, the AFM phase image (Fig. 6) displays lamellar structure. Also, in electron holography and conventional electron microscopy, we found similar spacing and shape of the lamellae (Figs. 7 and 8). A small discrepancy in the

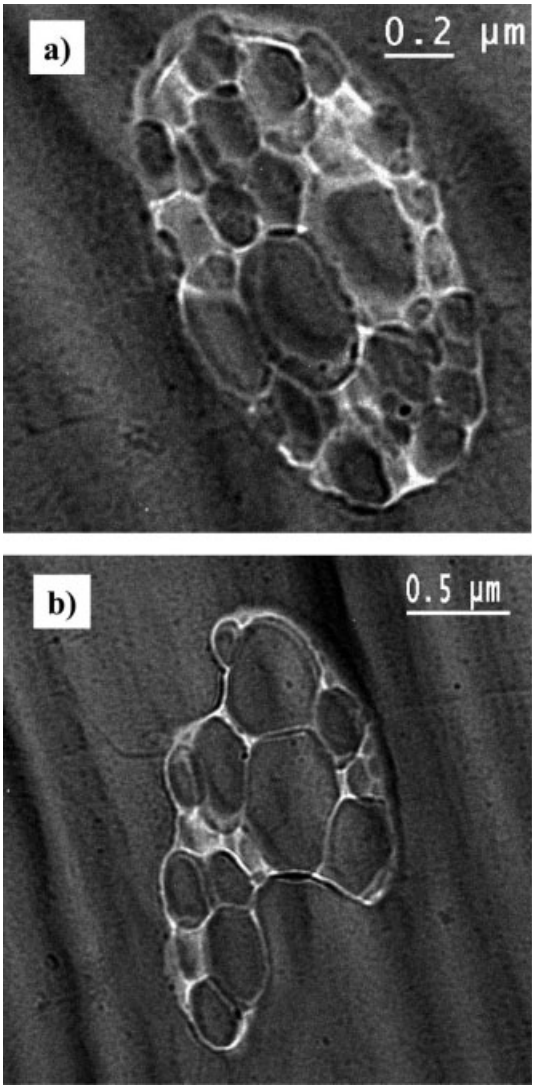

Figure 12 Lorentz electron micrographs of nonstained high impact polystyrene (HIPS). The diameter of the PS inclusions inside the particle (about 0.81–1.45 μm in diameter) lies between 70 and 450 nm.

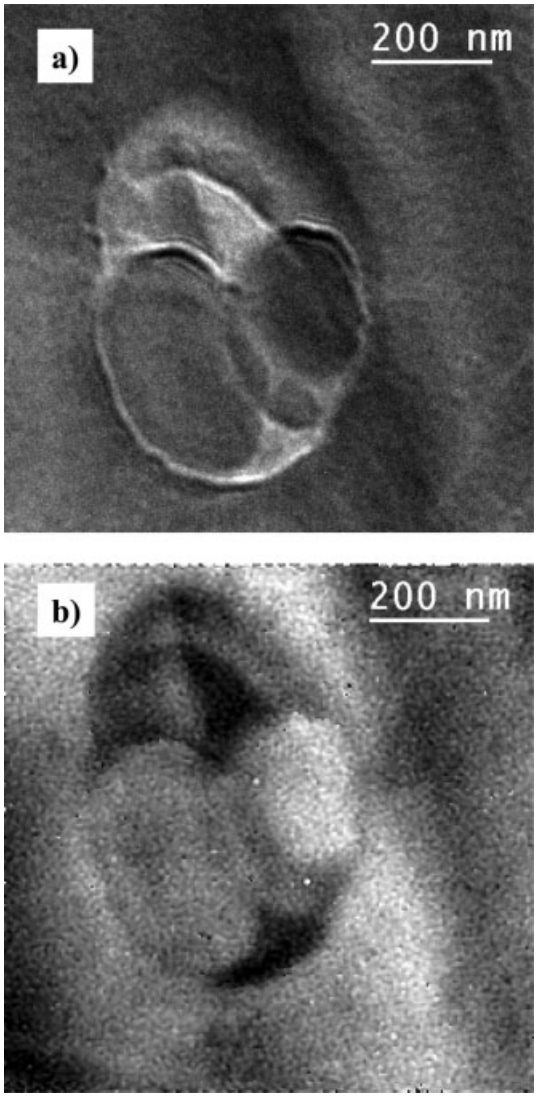

Figure 13 Lorentz electron micrograph (a) and electron phase image of reconstructed hologram (b) of the high impact polystyrene (HIPS) imaged at the same sample area.

periods measured by different methods results, on the one hand, from different sample positions investigated and, on the other hand, from the variable sensitivity of the techniques. For example, the variation of the lamellar period in the TEM images is in part due to the local variation of the lamellar normal with respect to the incident beam direction. Additionally, the AFM is sensitive to the surface topography whereas TEM averages through the total sample thickness of about 50–70 nm. As a consequence, in electron holography thickness variations and density modulations could be superimposed along the electron path and therefore may not be unambiguously differentiated. The hexagonal lattice as well as the parallel array of the polystyrene cylinders in SEBS-S30 were successfully imaged by the tapping mode atomic force microscopy [Fig. 9(a) and (b)].

A very good agreement in the structure of the HIPS was found by the AFM and the electron microscopy measurements. However, the micrographs recorded at strong defocus using conventional microscopy gave rise to the so called Fresnel fringes. These artifacts result in the appearance of pronounced white surroundings of the domains [Fig. 12(a) and (b)] thus reducing the theoretical point resolution of 2.2 nm of the Lorentz lens to 20 nm at least. The electron holograms are recorded in-focus thus avoiding the appearance of Fresnel fringes and exploiting the resolution limit for the Gabor focus (defined as $\times 0.56$ Scherzer focus) of 2.5 nm. However, in electron holography, one has to find a balance between lateral resolution and signal/noise ratio: the reason is that lateral resolution reconstructable from a hologram is given by twice the spacing of the hologram fringes, the signal/noise ratio is determined by the fringe contrast, which is usually decreasing with fringe spacing. In the case of HIPS, we used a fringe spacing of about 4.5 nm, giving a resolution of about 9 nm. The maximum field of view for holography in the Lorentz mode of about 600 nm could be doubled, if necessary, by decreasing the current of diffraction lens significantly and applying negative voltage.[33]

The contrast of the electron phase micrographs may be improved by using smoother samples, which eliminates the effect of sample thickness variation. Solution casting may serve as an alternative method of preparing block copolymer thin films for electron holography. One has to ensure, nevertheless, that the superstructure remains the same in the thin solution cast films as in the bulk material. Thin sections used in our experiments might have been deformed during the cutting process. As a consequence, waviness, ripples, and microscopic roughness of the sample surface are produced. It should be noted that the necessity of working near the edge of the specimen to include free space in the image does not imply tears and thickness variations (wedge shape cuts) as can be seen, e.g., in the Lorentz micrograph for SIS-S50 [Fig. 7 (b)] or phase image for HIPS [Fig. 13(b)].

To enhance the signal/noise ratio and to achieve a better sample stability against beam damage, one may use a cooling holder. In this way, the critical dose could be increased and smaller structures, e.g., interfacial width of polymer blends at nanometer scale would be accessible for electron holography. Of course, in this case, we have to apply high-resolution holography instead of Lorentz holography due to the limited resolution of the Lorentz lens.

As a final remark, it can be stated that electron holography certainly cannot replace the well-established conventional electron microscopy techniques. However, it should be stressed that this technique, which is not frequently used by polymer scientists up to now, may open new possibilities of characterizing

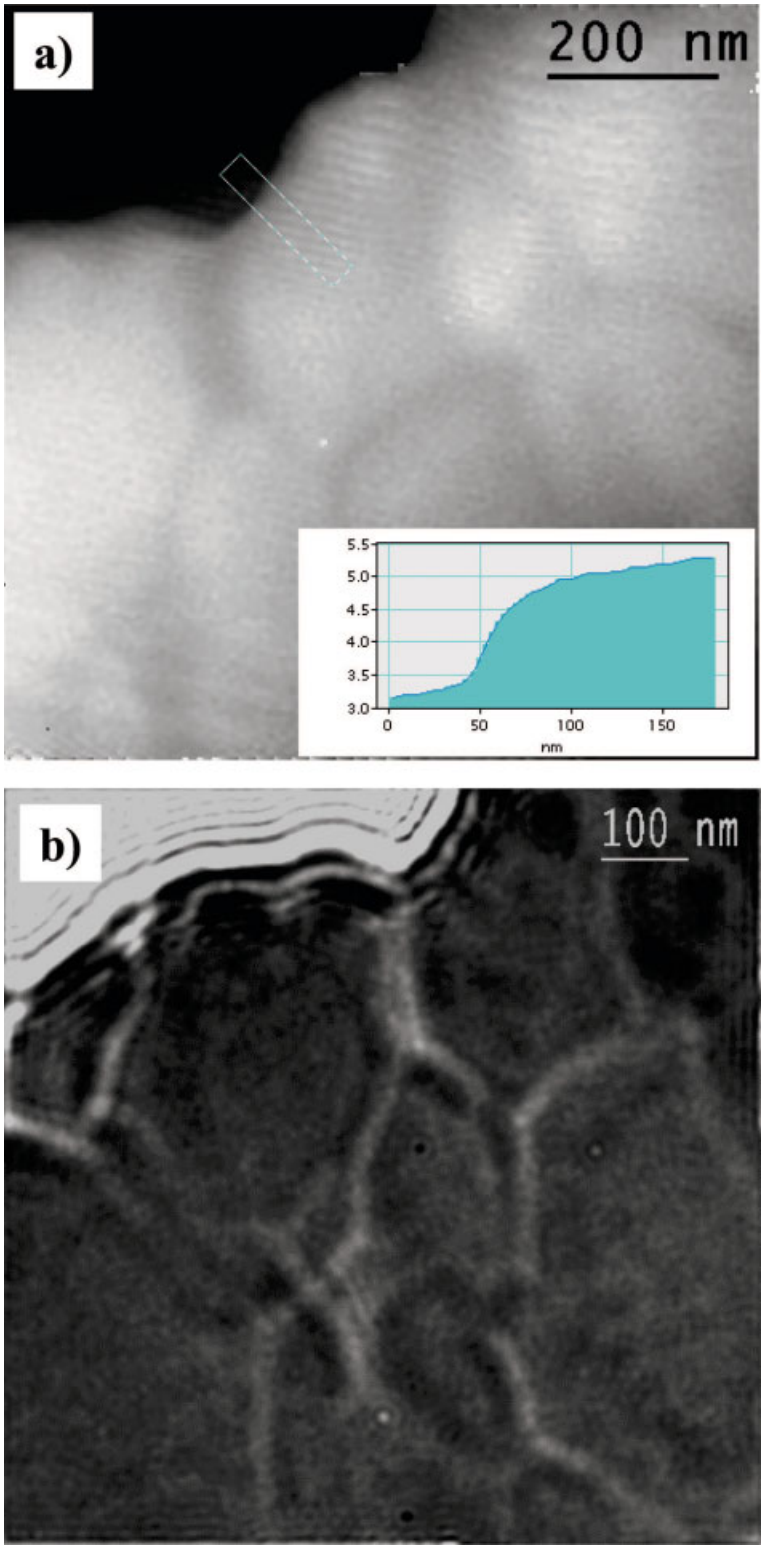

Figure 14 (a) Electron phase image of reconstructed hologram of the high-impact polystyrene (HIPS). The dark region at the top left corner is a vacuum. The bright polystyrene inclusions separated by narrow darker regions of polybutadiene are clearly visible. The phase shift due to PS amounts to 1.9 rad (inset at the right bottom) plus 2π, which results in a thickness of 137 nm assuming the inner potential to be 8.2 V. (b) Lorentz micrograph of HIPS recorded from about the same area as (a). The edge of the sample is showing strong blurring caused by the bright Fresnel fringes at large defocus.

structures of heterogeneous polymers. In particular, it could be an attractive alternative to image heterogeneous polymers, in which neither of the components are susceptible toward selective chemical staining by heavy metal compounds.

Our sincere acknowledgment goes to Mrs. Sylvia Goerlitz (Halle) for the preparation of ultrathin sections of the samples. R. A. thanks the Kultusministerium des Landes Sachsen-Anhalt and the Max-Buchner-Forschungsstiftung for financial support.

References

1. Lednicky, F.; Coufalova, E.; Hromadkova, J.; Delong, A.; Kolarik, V. Polymer 2000, 41, 4909.
2. Simon, P.; Huhle, R.; Lehmann, M.; Lichte, H.; Mönter, D.; Bieber, T.; Reschetilowski, W.; Adhikari, R.; Michler, G. H. Chem Mater 2002, 14, 1505.
3. Meyer, R. R.; Sloan, J.; Dunin-Borkowski, R. E.; Kirkland, A. I.; Novotny, M. C.; Bailey, S. R.; Hutchison, J. L.; Green, M. L. H. Science 2000, 289, 1324.
4. Völkl, E.; Allard, L. F.; Joy, D. C. Introduction to Electron Holography; Kluwer Academic/Plenum Publishers: New York, 1999.
5. Lichte, H. Phil R Trans Soc Lond A 2002, 360, 897.
6. Lichte, H.; Lehmann, M. Adv Imaging Electron Phys 2002, 123, 225.
7. Midgley, P. A. Micron 2000, 32, 167.
8. Lehmann, M.; Lichte, H. Microsc Microanal 2002, 8, 447.
9. Binh, V. T.; Semet, V.; Garcia, N. Ultramicroscopy 1995, 58, 307.
10. Wang, Y. C.; Chou, T. M.; Libera, M.; Voelkl, E.; Frost, B. G. Microsc Microanal 1998, 4, 146.
11. Harscher, A. Ph.D. Thesis, University of Tübingen, Germany 1999.
12. Chou T. M.; Libera, M.; Gauthier M. Polymer 2003, 44, 3037.
13. Wahlheim, S.; Schäfer, E.; Mlynek, J; Steiner, U Science 1999, 238, 520.
14. Schwark, D. W.; Vezie, D. L.; Reffner, J. R.; Thomas, E. L.; Annis, B. K. J Mater Sci Lett 1992, 11, 352.
15. Stocker, W.; Beckmann, J.; Stadler, R.; Rabe, JP. Macromolecules 1996, 29, 7502.
16. Elbs, H.; Fukunaga, K.; Stadler, R.; Sauer, G.; Magerie, R.; Krausch, G. Macromolecules 1999, 32, 1204.
17. Magonov, S.; Heaton, M. G. Am Lab 1998, 30, 9.
18. Galuska, A.; Pouter, R. R.; McEarlth, K. O. Surf Interface Anal 1997, 25, 418.
19. Adhikari, R. Ph.D. Thesis, University of Halle-Wittenberg, Germany, 2001.
20. Magonov, S. N.; Elings, V.; Whangbo, M. H. Surf Sci 1997, 375, 385.
21. van Dijk, M. A.; van den Berg, R. Macromolecules 1995, 28, 6773.
22. Godehardt, R.; Rudolph, S.; Lebek, W.; Goerlitz, S.; Adhikari, R.; Allert, E.; Giesemann, J; Michler, G. H. J Macromol Sci B 1999, 38, 817.
23. Ott, H.; Abetz, V.; Altstädt, V.; Thomann, Y.; Pfau, A. J Microsc 2002, 205, 106.
24. Reimer, L. Transmission Electron Microscopy; Springer-Verlag: Heidelberg, Germany, 1989.
25. Petermann, J; Gleiter, H. J Polym Sci Polym Phys Ed. 1975, 13 1939.
26. Hendlin, D. L. Jr.; Thomas, E. L. Macromolecules 1983, 16, 1514.
27. Lichte, H. Ultramicroscopy 1991, 38, 13.
28. McLean, R. S.; Sauer, B. B. Macromolecules 1997, 30, 8314.
29. Bucknall, C. B. J Microsc 2001, 201, 221.
30. Michler, G. H. Appl Spectrosc Rev 1993, 28, 327.
31. Tsuji, M. Electron Microscopy, in Comprehensive Polymer Science; Sir Allen, G.; Bevington, J. C., Eds.; Pergamon Press: Oxford, UK, 1990; Vol. 1, p 806.
32. Zweck, J.; Bormans B. Electron Optics Bull 1992, 132, 1.
33. Chapman, J. N.; Johnston, A. B.; Heydeman, L. J.; McVitie, S.; Nicholson, W. A. P.; Bormans, B. IEEE Trans Magn 1994, 30, 4479.
34. Personal communication with Formanek, P. 2003.